

**ABSTRACT**

Traditionally the verification on the bearing capacity of shallow foundation in a seismic situation is executed using a methodology based in the global safety factor concept. However, this isn't the methodology proposed by EC8-5. The methodology proposed by this standard is based in the partial safety factors method and uses an analytical formulation that takes into account some of the effects of the seismic action.

In this paper, in order to understand the differences between these two methodologies used to verify the safety of shallow foundations in a seismic situation, a parametric study is performed. In this study, collapse and “design” loads are obtained by considering interaction between vertical and horizontal loads (N – V) and interaction between vertical load and moment (V – M) in a shallow strip foundation without embedment. Also in this study, the verification on the bearing capacity of shallow foundations according to EC8-5 for a seismic situation is compared with the verification on the bearing capacity of shallow foundations according to EC7-1 for a static situation. In the end, numerical simulations of one of the cases analysed in the study are performed using FLAC software. These simulations were performed considering seismic action through a horizontal constant acceleration – pseudo – static analysis – and through an actual earthquake acceleration time history – dynamic analysis.

**1 . INTRODUCTION**

According to EC8-5, bearing capacity failure is one of the ultimate limit state of shallow foundations in a seismic situation. To check this ULS, Annex F of this standard proposes a general expression and criteria based in the bounding surface concept,

$$\phi(N, V, M, F) \leq 0 \tag{1}$$

Where  $\phi() = 0$  defines the equation of a bounding surface. Inequality 1 expresses the fact that any combination of the loading parameters N, V, M e F lying outside the surface corresponds to a collapse situation.

General expression of Annex F, has been derived from theoretical limit analysis of a strip footing and is applicable to cohesive and cohesionless soils. This expression takes into account the load inclination and eccentricity acting on the foundation, as well the effect of the soil inertia forces. Figure 1 presents the bounding surface proposed by Annex F of EC8-5 for cohesive soils.

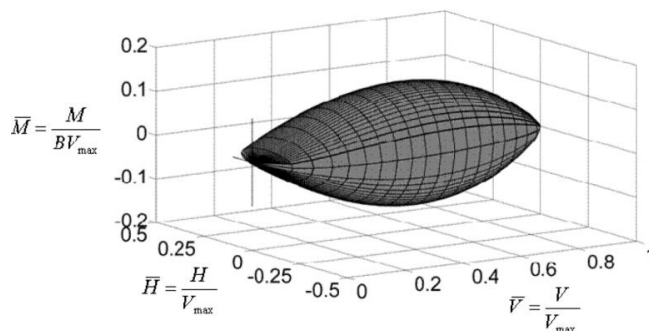


Figure 1 – EC8-5 bounding surface for cohesive soils.

**2 . SAFETY VERIFICATIONS OF SHALLOW FOUNDATIONS – Bearing capacity failure**

**2.1. Verifications based in the safety partial factors**

**2.1.1. Eurocode 7**

According to Eurocode 7 and considering the direct method, bearing capacity failure is one of the ultimate limit states for shallow foundations in a static situation.

To check this ULS the following inequation must be satisfied,

$$V_d \leq R_d \quad [2]$$

Where  $V_d$  and  $R_d$  are the design action and resistance respectively. The design action is obtained considering the fundamental combination,

$$E_d = E \left\{ \sum_{j \geq 1} \gamma_{Gj} G_{kj} + \gamma_{Qj} Q_{k1} + \sum_{i > 1} \gamma_{Qi} \psi_{0i} Q_{ki} \right\} \quad [3]$$

The design resistance is obtained through equations suggested in Annex D of Eurocode 7.

### 2.1.2. Eurocode 8

Eurocode 8 is divided in six parts. Part 5 establishes the requirements, criteria, and rules for the siting and foundation soil of structures for earthquake resistance. In this standard, regarding his behaviour, soil is classified in cohesive soil and cohesionless soil.

As mentioned previously, the bearing capacity failure of soil is, again, one of the ultimate limit states for a shallow foundation in a seismic situation. To check this ULS, EC8-5 suggests using the general expression and criteria provided in Annex F,

$$\frac{(1 - e\bar{F})^{c_T} (\beta\bar{V})^{c_T}}{(\bar{N})^a [(1 - m\bar{F}^k)^{k'} - \bar{N}]^b} + \frac{(1 - f\bar{F})^{c'_M} (\beta\bar{M})^{c'_M}}{(\bar{N})^c [(1 - m\bar{F}^k)^{k'} - \bar{N}]^d} - 1 \leq 0 \quad [4]$$

Where,

$$\bar{N} = \frac{\gamma_{RD} N_{Ed}}{N_{m\acute{a}x}} \quad \bar{V} = \frac{\gamma_{RD} V_{Ed}}{N_{m\acute{a}x}} \quad \bar{M} = \frac{\gamma_{RD} M_{Ed}}{BN_{m\acute{a}x}} \quad [5]$$

$N_{m\acute{a}x}$  – is the ultimate bearing capacity of the foundation under a vertical centred load;

$B$  – is the foundation width;

$\bar{F}$  – is the dimensionless soil inertia force;

$\gamma_{RD}$  – is the model partial factor;

$a, b, c, d, e, f, m, k, k', c_T, c'_M, c'_M, \beta, \gamma$  – Numerical parameters depending on the type of soil.

Table 1 – Values of numerical parameters used in expression 4.

	$a$	$b$	$c$	$d$	$e$	$f$	$m$	$k$	$k'$	$c_T$	$c_M$	$c'_M$	$\beta$	$\gamma$
Cohesive soils	0.70	1.29	2.14	1.81	0.21	0.44	0.21	1.22	1.00	2.00	2.00	1.00	2.57	1.85
Cohesionless soils	0.92	1.25	0.92	1.25	0.41	0.32	0.96	1.00	0.39	1.14	1.01	1.01	2.90	2.80

For purely cohesive soils or saturated cohesionless soil the ultimate bearing capacity under a vertical concentric load  $N_{max}$  is given by,

$$N_{max} = (\pi + 2) \frac{\bar{c}}{\gamma_M} B \quad [6]$$

$\bar{c}$  – Undrained shear strength of soil for cohesive soil,  $c_u$ , or the cyclic undrained shear strength,  $\tau_{cy,u}$ , for cohesionless soils;

$\gamma_M$  – Partial factors for material proprieties.

The dimensionless soil inertia force  $\bar{F}$  is given by,

$$\bar{F} = \frac{\rho a_g S B}{c_u} \quad [7]$$

$\rho$  – Unit mass of soil;

$a_g$  – Design ground acceleration on type A ground;

$S$  – Soil factor defined in EN 1998 – 1:2004.

The following constraints apply to general bearing capacity expression,

$$0 < \bar{N} \leq 1, |\bar{V}| \leq 1 \quad [8]$$

For purely dry cohesionless soils or for saturated cohesionless soils without significant pore pressure building, the ultimate bearing capacity of the foundation under a vertical centred load  $N_{max}$  is given by

$$N_{max} = \frac{1}{2} \rho g \left( 1 \pm \frac{a_v}{g} \right) B^2 N_\gamma \quad [9]$$

$g$  – acceleration of gravity;

$a_v$  – vertical ground acceleration, that may be taken as being equal to  $0.5a_g \cdot S$ ;

$N_\gamma$  – Bearing capacity factor.

The dimensionless soil inertia force  $\bar{F}$  is given by,

$$\bar{F} = \frac{a_g}{g \tan(\phi'_d)} \quad [10]$$

$\phi'_d$  – Design angle of the shearing resistance of soil.

The following constraints apply to general bearing capacity expression,

$$0 < \bar{N} \leq (1 - m\bar{F})^{k'} \quad [11]$$

For cohesive soils and in most common situations, Annex F suggests ignore soil inertia forces. For cohesionless soils soil inertia forces may be neglected if  $a_g \cdot S < 0.1g$ .

Table 2 shows the values of the model partial factor  $\gamma_{RD}$ . This factor is introduced to reflect the uncertainties in the theoretical model.

Table 2 – Values of the model partial factor  $\gamma_{RD}$ .

Medium – dense to dense sand	Loose dry sand	Loose saturated sand	Non sensitive clay	Sensitive clay
1,00	1,15	1,50	1,00	1,15

In this paper, the model partial factor  $\gamma_{RD}$  was considered equal to 1.15 for cohesionless soils (loose dry sands) and equal to 1 for cohesive soils (non sensitive clays).

For the design seismic situation, the design action is obtained considering the seismic combination,

$$E_d = E \left\{ \sum_{j \geq 1} G_{kj} + A_{ed} + \sum_{i \geq 1} \psi_{2,i} Q_{ki} \right\} \quad [12]$$

where  $G_{kj}$  represents the characteristic value of a permanent action,  $A_{ed}$  the design value of a seismic action and  $\psi_{2,i} Q_{ki}$  the quasi-permanent value of variable action  $i$ . In this paper, the value considered for  $\psi_{2,i}$  was 0.3. Tables 3 and 4 shows the partial safety factors to adopt in a seismic design situation. For this design situation only one calculation approach is needed. According to EC8-5 National Annex, the partial safety factors for the soil parameters are equal to the soil parameters indicated by the EC7-1 National Annex for accidental situations.

Table 3 - Safety partial factors for actions in a seismic design situation.

Action	Symbol	
Permanent	Unfavourable	1,0
	Favourable	$\gamma_G$ 1,0
Variable	Unfavourable	1,0
	Favourable	$\gamma_Q$ 1,0

Table 4 – Safety partial factors for soil parameters in a seismic design situation.

	Symbol	
Angle of shearing resistance	$\gamma_{\phi'}$	1,1
Effective cohesion	$\gamma_{c'}$	1,1
Undrained shear strength	$\gamma_{c_u}$	1,15
Unconfined strength	$\gamma_{qu}$	1,15

## 2.2. Verification based in the global safety factor (GFS)

### 2.2.1. "Traditional" methodology

Traditionally, the design of shallow foundations is executed using a methodology based in the global safety factor concept – GSF. According to this methodology, the designer must ensure that the acting stress on soil foundation is lower than the allowable bearing capacity of soil. Allowable bearing capacity is obtained dividing the ultimate bearing capacity of soil by a global safety factor as suggested in equation 13.

$$q_{all} = \frac{q_{ult}}{GSF} \quad [13]$$

In equation 13,  $q_{all}$ ,  $q_{ult}$  and  $GSF$  represents, respectively, the allowable bearing capacity, the ultimate bearing capacity and the global safety factor. The ultimate bearing capacity of soil can be obtained through one of the multiple methods existing in literature. In this paper, the global safety factor considered for cohesive and cohesionless soils was 2 and 3, respectively.

This methodology is also applied to a seismic situation. For this situation, the allowable stress of soil is obtained increasing the static value by percentages ranging from 20% to 50%. This increasing of the allowable soil stress is related with the lower probability of occurrence of a seismic event and can be seen like a reduction in the global safety factor.

## 3. PARAMETRIC STUDY

### 3.1 Methodology

In this parametric study, three comparisons were performed:

1. Comparison of collapse loads for a static and seismic situation obtained from analytical formulation proposed in Annex D of EC7-1 and Annex F of EC8-5 respectively.
2. Comparison of design loads for a static and seismic situation obtained according EC7-1 and EC8-5, respectively.
3. Comparison of design loads for a seismic situation obtained according EC8-5 and according the "traditional" approach.

Collapse and design loads were obtained considering a shallow strip foundation under eccentric and inclined loading in cohesive and cohesionless soils. Different foundations widths,  $a_g/g$  relations and soils parameters were adopted. Figure 2 illustrate the cases considered, while table 5 shows the parameters used in this study with their respective ranges of variation. In this paper, only the results obtained for the foundation with width  $B = 1$  m,  $\Phi' = 25^\circ$  and  $c_u = 50$  kPa are presented.

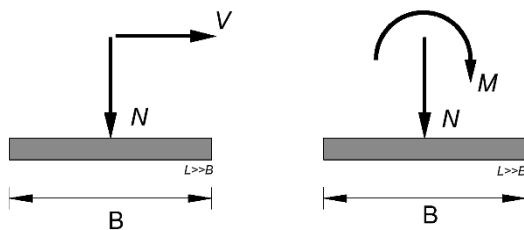


Figure 2 - Shallow strip foundation under eccentric and inclined loading.

Table 5 - Parameters considered in this analysis and respective values.

B (m)	$\gamma$ (kN/m <sup>3</sup> )	$c_u$ (kPa)	$\Phi'$ (°)
1,2 e 4	20	50 e 200	25 e 35

Note that, for the Eurocodes verifications, the term design load is referring to the characteristic value of the permanent action that checks the ULS of bearing capacity failure. For the "traditional" methodology, this load corresponds to the permanent value of the acting load that checks bearing capacity failure verification –  $q_{acting} \leq q_{all} \times (1.2 \text{ a } 1.5)$

### 3.2 Comparison of collapse loads – Static and seismic situation

Figures 3 and 4 presents static and seismic collapse loads obtained from analytical formulation proposed in Annex D of EC7-1 and on Annex F of EC8-5 respectively. These loads were obtained for both cohesive and cohesionless soils.

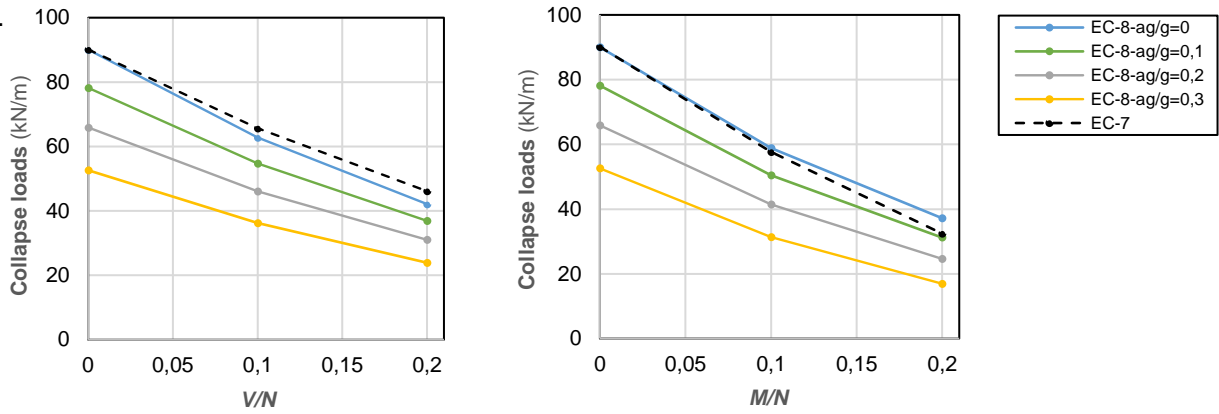


Figure 3 - Collapse load values obtained for N – V and N – M interaction situations – B = 1 m and  $\phi' = 25^\circ$

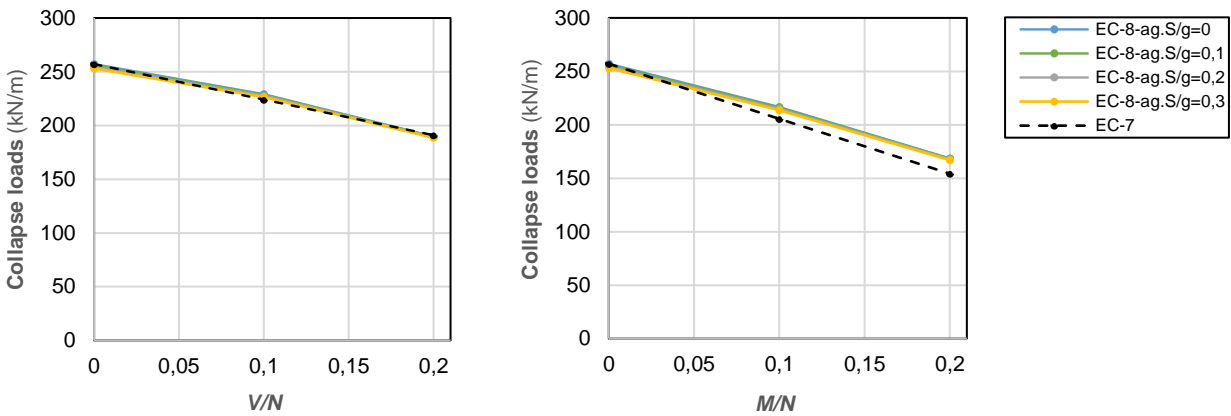


Figure 4 - Collapse load values obtained for N – V and N – M interaction situations – B = 1 m and  $c_u = 50$  kPa.

Figures 3 and 4 shows that both static and seismic collapse loads are reduced by eccentricity and inclination of the loading. For cohesionless soils, seismic collapse loads are also reduced by horizontal acceleration. For cohesive soils, collapse load values aren't affected by horizontal acceleration.

### 3.3 Comparison of design loads – Static and seismic situation

Figures 5 and 6 present static and design loads obtained according EC7-1 and EC8-5 respectively. This figures shows that until values of  $a_g/g$  between 0.2 and 0.3, and for the same values of eccentricity and inclination, the static design loads are always lower than the seismic design loads. For higher values of  $a_g/g$ , the situation changes, and the seismic design loads are lower than the static design loads. For cohesive soils, due to difference between the static and seismic partial safety factors, the static design loads are always lower than seismic design loads.

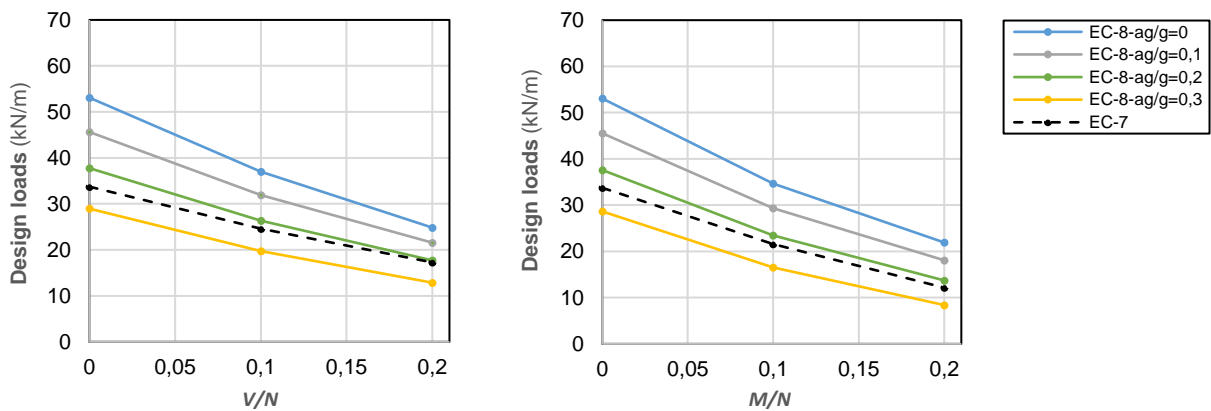


Figure 5 – Design loads values obtained for N – V and N – M interaction situations – B = 1 m and  $\phi' = 25^\circ$ .

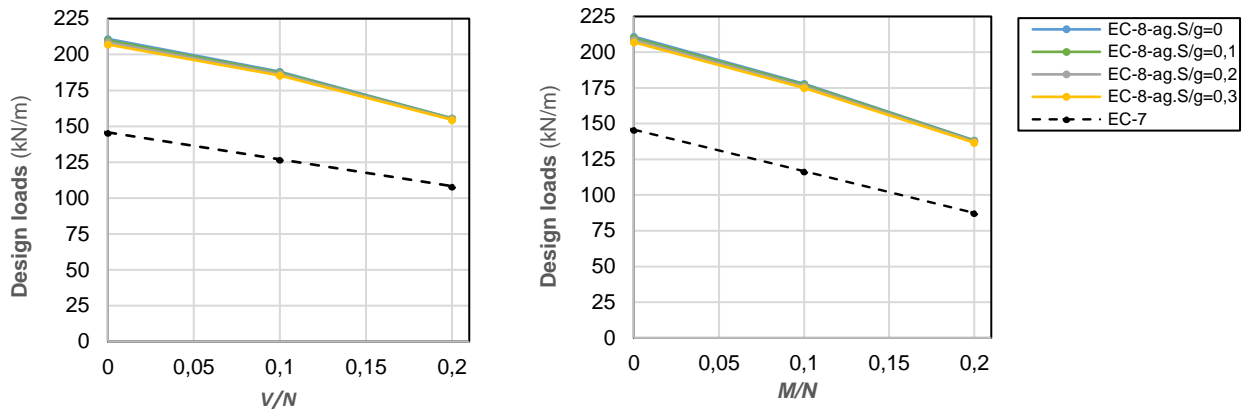


Figure 6 – Design loads values obtained for N – V and N – M interaction situations – B = 1 m and  $c_u = 50$  kPa.

### 3.4 Comparison of design loads – Seismic situation

Figure 7 and 8 shows the design loads for a seismic situation obtained according EC8-5 and according traditional design methodology – GSF (global safety factor) – presented earlier. Notice that when applying this design methodology, two sets of loads are obtained. This two sets corresponds to the admissible loads increased in 20% and 50 %.

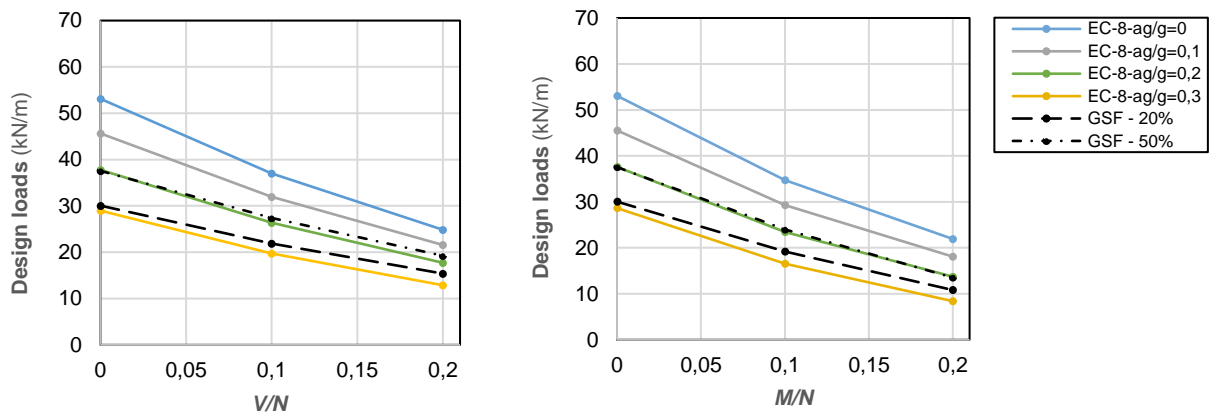


Figure 7 - Design loads values obtained for N – V and N – M interaction situations – B = 1 m and  $\phi' = 25^\circ$ .

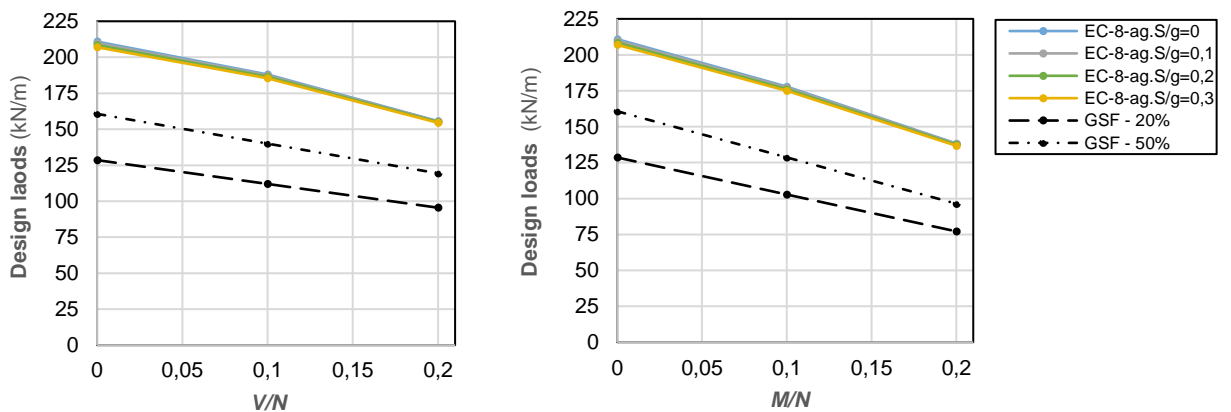


Figure 8 - Design loads values obtained for N – V and N – M interaction situations – B = 1 m and  $c_u = 50$  kPa.

Figures 7 and 8 shows that, for cohesionless soils, until values of  $a_g/g$  very close to 0.2, design loads obtained according the “traditional” methodology are lower than the design loads obtained according

EC8-5. For cohesive soils, and for all  $a_g/g$  values considered, the design loads obtained according the “traditional” methodology are always lower than the design loads obtained according to EC8-5.

## 4. NUMERICAL SIMULATIONS

### 4.1 Pseudo-static simulations

In pseudo-static simulations seismic collapse loads were again obtained for a shallow strip footing without embedment under eccentric and inclined loading. These loads were obtained for both cohesive and cohesionless soils.

#### 4.1.1. Numerical model

Discretization, geometry and the boundaries conditions considered in the numerical model are shown in Figure 9-a). The footing is strip, without embedment and of width  $B = 1$  m. The height  $H$  and the length  $L$  of the discretized domain are  $10B$  and  $20B$ , respectively. The base of the model is constrained in all directions, while the right and the left vertical sides are constrained only in the horizontal direction. The numerical model is discretized into elements with different sizes. Near the zone where the footing load is applied, the square elements of the mesh have  $0.05$  m aside whereas far from this region, the elements are bigger, with  $0.2$  m aside.

Collapse loads were obtained by applying a downward velocity to the gridpoints representing the footing (Figure 9 b)). This constant downward velocity applied simulate the footing load. For this type of simulation, seismic loading was considered as a horizontal constant acceleration.

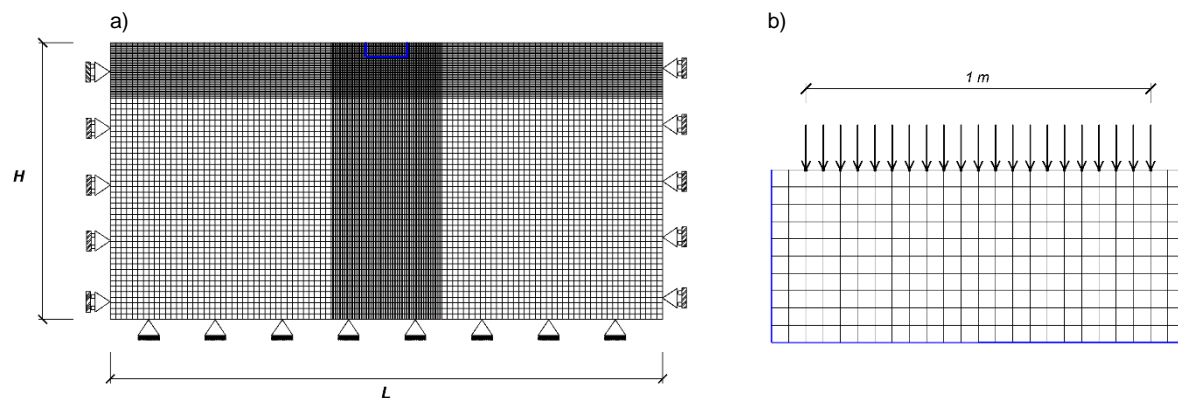


Figure 9 – Representation of the numerical model – a) and numerical procedure – b) used in pseudo – static analysis.

The soil was modelled as an elastic perfectly plastic material obeying Mohr-coulomb failure criteria for cohesionless soils, and Tresca failure criteria for cohesive soils. Table 6 presents the soils parameters considered in all numerical simulations for both type of soils.

Table 6 – Soil parameters considered in numerical analysis.

	$\nu$	$E$ (MPa)	$\phi'$ ( $^\circ$ )	$c_u$ (kPa)	$\Psi$ ( $^\circ$ )
Cohesionless soil	0.3	20	25	-	25
Cohesive soil	0.45	20	-	50	-

#### 4.1.2. Collapse loads

Figures 10 and 11 shows the seismic collapse loads obtained from pseudo-static numerical simulations. For cohesionless soils, collapse loads are reduced by horizontal acceleration while for cohesive doesn't. For this type of soils, the collapse loads obtained for different values of  $a_g/g$  are practically the same.

Notice that in both figures, collapse loads obtained analytically (through Annex F general expression) are also presented. Once this is an upper bound solution, collapse loads obtained from this expression should always be higher than numerically obtained collapse loads. However, this isn't always verified.

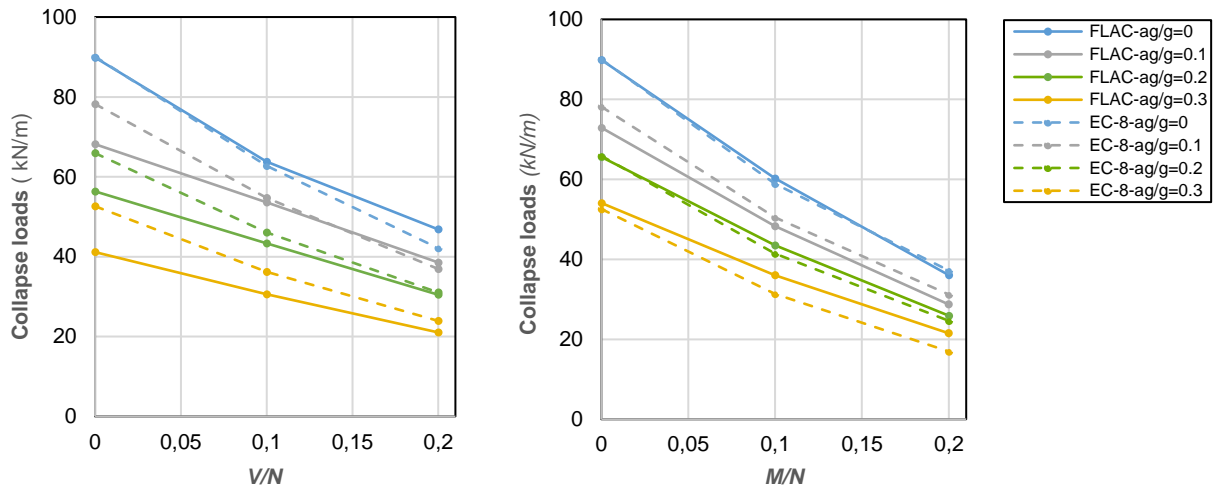


Figure 10 – Collapse loads obtained numerically and through Annex F general expression –  $B = 1 \text{ m}$  e  $\Phi' = 25^\circ$ .

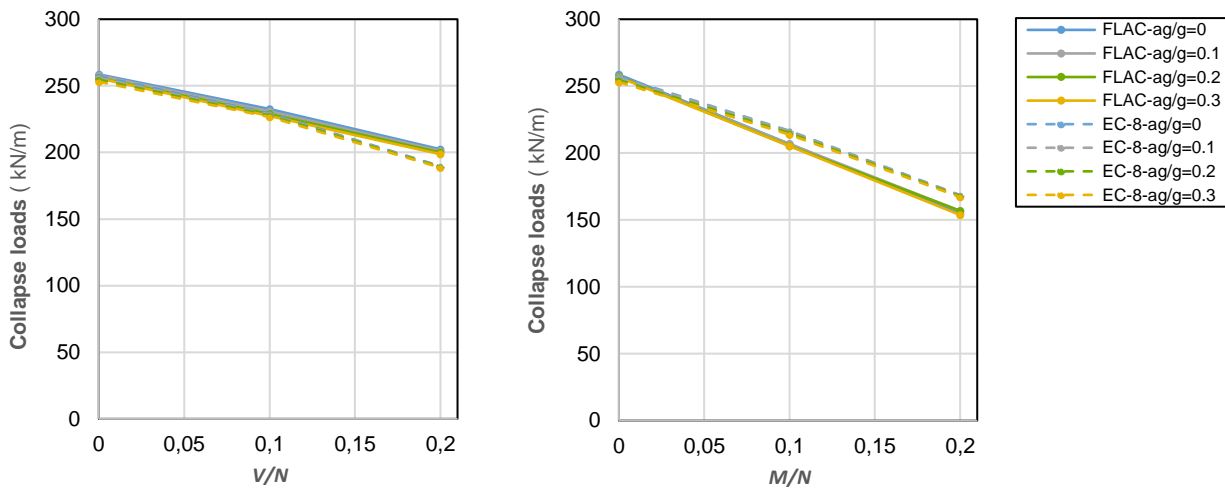


Figure 11 – Collapse loads obtained numerically and through Annex F general expression –  $B = 1 \text{ m}$  e  $c_u = 50 \text{ kPa}$ .

## 4.2 Dynamic simulations

In dynamic simulations vertical displacements were obtained for the strip footing of width  $B = 1 \text{ m}$  under vertical loading and for  $a_g/g$  equal to 0.1, 0.2 and 0.3. This time, an actual seismic record was used to simulate the seismic action. In order to obtain the different values of  $a_g/g$  in the foundation's base this record was scaled.

### 4.2.1. Numerical model

The numerical model used in dynamic analysis was similar to the model presented in Figure 9 with some differences. For this type of analysis, free – field boundaries and Rayleigh's type of damping were also considered. In order to obtain the vertical displacements of the foundations, seismic collapse loads were applied followed by seismic action. These loads correspond to the loads presented in Figures 3 and 4 for  $M/N = 0$  and  $V/N = 0$  and are shown in table 7.

Figure 12 shows the seismic record used to simulate the seismic action. This record is representative of the 1987 Loma Prieta earthquake in California, and only the record between  $t = 3.5 \text{ s}$  and  $t = 5.0 \text{ s}$  was used in these simulations.



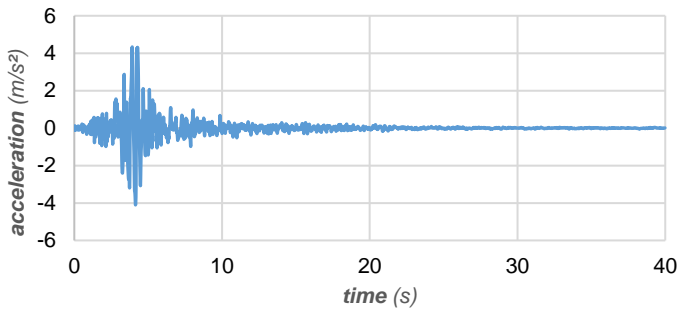


Figure 12 - Seismic record of Loma Prieta earthquake

Table 7 - Collapse loads applied in dynamic simulations.

	Cohesionless Soils	Cohesive Soils
$a_g/g = 0,1$	78,2 kN/m	256 kN/m
$a_g/g = 0,2$	65,9 kN/m	254,6 kN/m
$a_g/g = 0,3$	52,6 kN/m	253 kN/m

Figure 13 shows the vertical displacements obtained in the end (when time = 2,5 s) of dynamic simulations for cohesionless and cohesive soils. Notice that, for the initial moment  $t = 0$ , the vertical displacement is different from 0 and correspond to the displacement caused by the application of the collapse load. For both type of soils, the application of the seismic action increases the vertical displacement of the foundation.

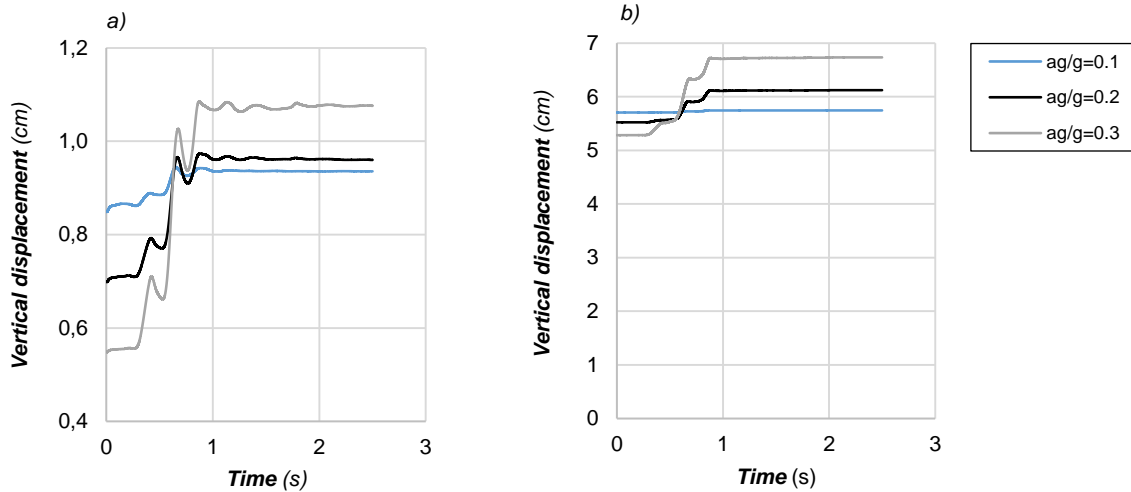


Figure 13 - Vertical displacements of the foundation during simulations - a) cohesionless soils b) cohesive soils.

Figures 14 and 15 shows load – displacement curves obtained in pseudo-static conditions for the same strip footing of width  $B = 1$  m and for  $a_g/g = 0.1, 0.2$  e  $0.3$ . Introducing in these curves, the vertical displacements presented in Figure 13, it can be seen that these are very close to the displacements for whom the foundation reaches collapse.

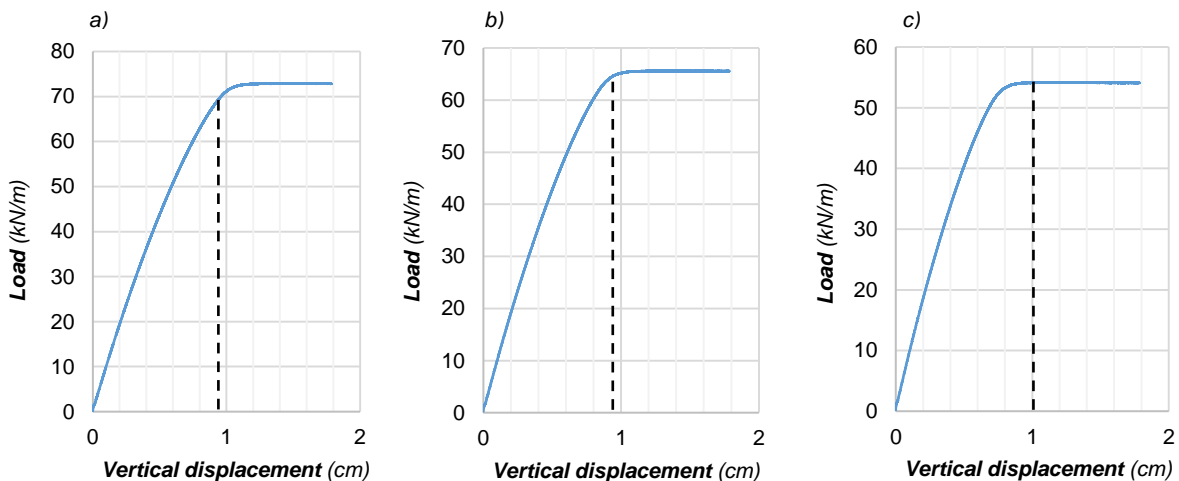


Figure 14 – Load – displacement curves for cohesionless soils –  $B = 1.0$  m e  $\Phi' = 25^\circ$  – a)  $a_g/g = 0.1$  b)  $a_g/g = 0.2$  c)  $a_g/g = 0.3$

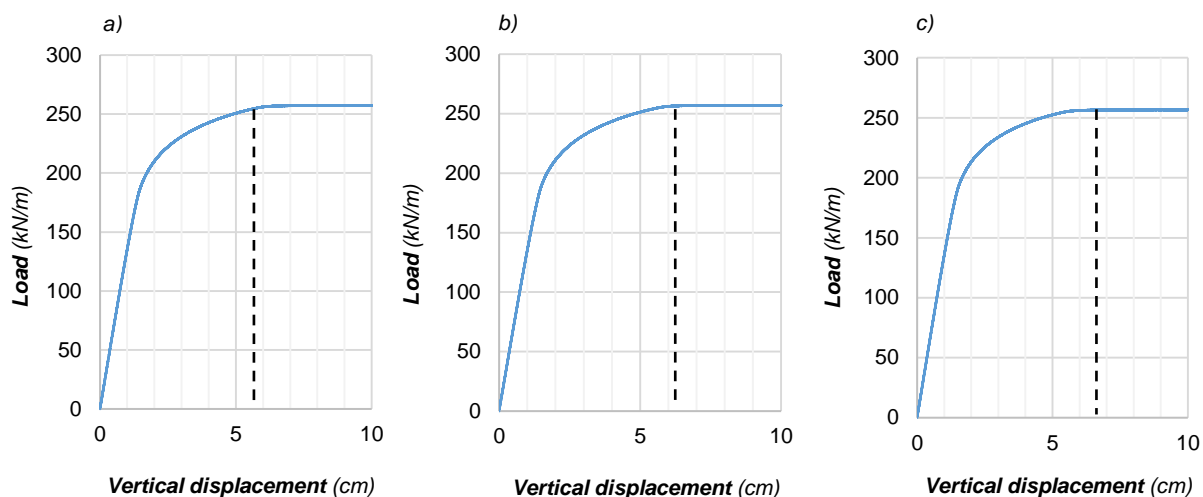


Figure 15 – Load – displacement curves for cohesive soils –  $B = 1.0 \text{ m}$  e  $c_u = 50 \text{ kPa}$  – a)  $a_g/g = 0.1$  b)  $a_g/g = 0.2$  c)  $a_g/g = 0.3$

----- Vertical displacements obtained in the end of the dynamic simulations.

## 5. CONCLUSIONS

The differences between the verifications on the bearing capacity of shallow foundations for a seismic situation according the EC8-5 and the “traditional” methodology were analysed through a parametric study. The results of this study indicate that, for cohesionless soils, and until values of  $a_g/g = 0,2$ , the methodology based in the global safety factor concept is more conservative. For cohesive soils, this methodology, is always more conservative. For this type of soil, large differences between design loads were obtained mainly because of the difference between the global safety factor used in traditional methodology and the partial safety factor for undrained strength ( $\gamma_{cu}$ ) used in EC8-5 design methodology.

Numerical simulations, for the strip footing without embedment and of width  $B = 1 \text{ m}$ , using FLAC software were also performed. Pseudo-static results are in good agreement with Annex F general expression, while vertical displacements obtained in dynamic simulations indicates that, even in dynamic conditions, this expression provides good estimations of seismic collapse loads.

## REFERENCES

- Eurocode NP EN 1997-1:2010 – *Geotechnical design - Part 1: General rules.*
- Eurocode NP EN 1998-1:2010 – *Design of structures for earthquake resistance - Part 1: General rules, seismic actions and rules for buildings.*
- Eurocode NP EN 1998-1:2010 – *Design of structures for earthquake resistance - Part 5: Foundations, retaining structures and geotechnical aspects.*
- Pecker, A. (1997). Analytical formulae for the seismic bearing capacity of shallow strip foundations. *Seismic behaviour of Ground and Geotechnical Structures, Sêco e Pinto.*
- Pecker, A. (2011). Design of concrete foundation elements. *Eurocode 8: Seismic Design of Buildings – Worked examples.* Lisboa, Portugal, pp. 84-104
- Puri, V. and Prakash, S. (2007) Foundations for Seismic Loads. *Proceedings of Geo-Denver 2007, Dynamic Response and Soil Properties.* Denver, USA, pp. 1-10.
- Tiznado A., Paillao V. (2014). Analysis of the seismic bearing capacity of shallow foundations, *Revista de la Construcción*, vol.13, n.2, pp. 40-48.
- Toh, J.C.W., Pender, M.J. (2010) Design approaches and criteria for earthquake-resistant shallow foundations systems, *Soil – Foundation – Structure - Interaction, Orense, R.P., Chow, N., Pender, M.J.*
- Sereno, P.M. (2016). Dimensionamento sísmico de fundações superficiais. Master's degree thesis dissertation, Instituto Superior Técnico, University of Lisbon.